Translational Oncology
www.transonc.com

Volume 12 Number 2 February 2019 pp. 217–225 217

Attenuation of CD47-SIRPα Signal in Cholangiocarcinoma Potentiates Tumor-Associated Macrophage-Mediated Phagocytosis and Suppresses Intrahepatic Metastasis[1,2]

Kulthida Vaeteewoottacharn[*,†,‡], Ryusho Kariya[*], Phattarin Pothipan[†,‡], Sawako Fujikawa[*], Chawalit Pairojkul[‡,§], Sakda Waraasawapati[‡,§], Kazuhiko Kuwahara[¶], Chaisiri Wongkham[†,‡], Sopit Wongkham[†,‡] and Seiji Okada[*]

[*]Division of Hematopoiesis, Center for AIDS research and Graduate School of Medical Sciences, Kumamoto University, Kumamoto, Japan; [†]Department of Biochemistry, Faculty of Medicine, Khon Kaen University, Khon Kaen, Thailand; [‡]Cholangiocarcinoma Research Institute, Khon Kaen University, Khon Kaen, Thailand; [§]Department of Pathology Faculty of Medicine, Khon Kaen University, Khon Kaen, Thailand; [¶]Department of Diagnostic Pathology, Fujita Health University School of Medicine, Toyoake, Japan

Abstract

The involvement of chronic inflammation in cholangiocarcinoma (CCA) progression is well established. Cluster of differentiation 47 (CD47) is mutually expressed in various cancers and serves as a protective signal for phagocytic elimination. CD47 signaling blockage is a recent treatment strategy; however, little is known regarding CD47 in CCA. Therefore, the potential use of CD47 targeting in CCA was focused. CD47 was highly expressed in CCA compared to hepatocellular carcinoma (HCC). Disturbance of CD47-signal regulatory protein-α (SIRPα) interaction by blocking antibodies promoted the macrophage phagocytosis. The therapeutic potential of anti-CD47 therapy was demonstrated in liver metastatic model; alleviation of cancer colonization together with dense macrophage infiltrations was observed. The usefulness of anti-CD47 was emphasized by its universal facilitating macrophage activities. Moreover, increased production of inflammatory cytokines, such as IL-6 and IL-10, in macrophage exposed to CCA-conditioned media suggested that CCA alters macrophages toward cancer promotion. Taken together, interfering of CD47-SIRPα interaction promotes macrophage phagocytosis in all macrophage subtypes and consequently suppresses CCA growth and metastasis. The unique overexpression of CD47 in CCA but not HCC offers an exceptional opportunity for a targeted therapy. CD47 is therefore a novel target for CCA treatment.

Translational Oncology (2019) 12, 217–225

Introduction

Cluster of differentiation 47 (CD47) is a transmembrane glycoprotein that expresses ubiquitously on the surfaces of various cell types [1]. Among numerous roles, CD47 plays a substantial role in the immune surveillance [2,3]. CD47 is a marker of self-cells that is useful for the discrimination of host cells from damaged or foreign cells [4]. The interaction between CD47 and signal regulatory protein alpha (SIRPα) on phagocytic cell serves as an inhibitory signal for phagocytosis, and therefore, CD47 is termed "don't eat me" or antiphagocytic signal [2]. Emerging roles of CD47 in cancer have been revealed. The increase expression of CD47 protects cancer from

Address all correspondence to: Seiji Okada, MD, PhD, Division of Hematopoiesis, Center for AIDS research and Graduate School of Medical Sciences, Kumamoto University, 2-2-1 Honjo, Kumamoto, 860-0811, Japan. E-mail:okadas@kumamoto-u.ac.jp

[1] Declarations of Interest: none.

[2] Funding: This work was supported by a Grant-in-Aid for Scientific Research from the Ministry of Education, Culture, Sport Science and Technology (MEXT) of Japan (grant number 16K08742); the Tokyo Biochemical Research Foundation of Japan and Nakajima Heiwa Foundation (to S.O. and K.V.); Khon Kaen University, Thailand (#KKU601803 to K.V.); and Faculty of Medicine, Khon Kaen University, Thailand (#I57328 to K.V.).

Received 14 August 2018; Revised 14 October 2018; Accepted 16 October 2018

1936-5233/19
https://doi.org/10.1016/j.tranon.2018.10.007

immune surveillance [5–7]. Interfering of CD47-SIRPα interaction has demonstrated potential uses in various cancer treatments [5–8].

Cholangiocarcinoma (CCA) is a cancer of liver, arising from bile duct epithelia. It is a rare cancer worldwide, but increasing incidences have been observed [9,10]. CCA is a major health problem in Thailand, where the highest incidences and mortalities are documented [11]. The close association between CCA and chronic infection or chronic inflammation, regardless of the cancer causes, was reported [12]. Increased infiltrating macrophages and increased inflammatory mediators (e.g. IL-6, IL-8, IL-17RA, and IL-33) are associated with worsening prognosis of CCA patients [13–18]. Late diagnosis and poor response to conventional treatments are the major problems in CCA management [19,20]. Surgical resection is the only option that offers a curative outcome. However, only 20–40% of patients are candidates [21]. Recent advances of targeted therapy are expanding the options for CCA treatment. Immune checkpoint therapy is of our interest; however, recent reports of programmed death-ligand 1 (PD-L1) expression in CCA tissues were not encouraging. Infrequent or weak PD-L1 expression was reported in CCA from Thai and French patients [22,23]. Therefore, alternative pathway for macrophage modulation was studied to find a potential therapeutic strategy.

Recent advancement of immune checkpoint therapy has provided a promising result for cancer treatment. However, current reports on PD-L1 expression in CCA do not favor a PD-1/PD-L1-targeting clinical trial. Therefore, the innate immune surveillance protection, "don't eat me signal", was focused on, but the information regarding CD47 in CCA remains limited [24]. In the current study, CD47 expressions were determined in CCA tissues and cell lines compared to hepatocellular carcinoma (HCC). The potential use of CD47-SIRPα blocking for CCA treatment was investigated.

Materials and Methods

Cancer Tissues

Formalin-fixed paraffin-embedded tissues were obtained from the specimen bank of the Cholangiocarcinoma Research Institute, Khon Kaen University, Thailand. Seventy-six tissues (54 CCAs and 22 HCCs) were histologically proven. Written informed consent was obtained. The study protocol was reviewed and approved by the Ethical Committee for the Human Research of Khon Kaen University (HE571283 and HE571481) based on the Declaration of Helsinki.

Cell Lines

Four CCA cell lines, KKU-100, KKU-055, KKU-213, and HuCCT1, and two HCC cell lines, HepG2 and Huh7, were selected for the current study. CCA cell lines were obtained from the Japanese Collection of Research Bioresources Cell Bank (Osaka, Japan); HepG2 and Huh7 were kindly provided by Prof. Kyoko Tsukiyama-Kohara (Kagoshima University, Japan). Cells were maintained in RPMI1640 (Wako, Osaka, Japan) or DMEM (Wako) as recommendation. All media were supplemented with 10% FBS (HyClone, UT, USA), 100 U/ml penicillin, and 100 μg/ml streptomycin otherwise specified in the protocols. The cultures were maintained at 37°C in a humidified 5% CO_2 atmosphere.

Reagents and Antibodies

Human monocyte colony-stimulated factor (M-CSF) was a gift from Morinaga Milk Industry (Kanagawa, Japan). Lipopolysaccharide (LPS) was from Sigma-Aldrich (MO, USA). Granulocyte-monocyte colony-stimulated factor (GM-CSF), interferon-γ (IFN-γ), and interleukin-4 (IL-4) were from R&D system (MN, USA). Carboxyfluorescein diacetate succinimidyl ester (CFSE) and Hoechst 33342 were from Molecular Probe (OR, USA).

Sources of antibodies were as followed; anti–CD14-phycoerythrin (PE) (HCD14), anti–CD86-PE (IT2.2), anti–CD163-PE (GHI/61), anti–CD172a-PE (SIRPα/β) (SE5A5), anti–CD206-fluorescein isothiocyanate (FITC) (MMR, 15-2), anti–HLA-DR-FITC (L243), anti-F4/80 (CI: A3-1), and anti-CD172a (SE5A5) were from Biolegend (CA, USA); anti–CD47-FITC (2D3) and anti-CD47 (2D3) was from eBioscience (CA, USA); anti-CK19 (HPA002465) was from Sigma-Aldrich; Human Fc receptor blocking reagent was from Miltenyi Biotec (Bergisch Gladbach, Germany), isotype control antibodies were from Biolegend and DakoCytomation (Glostrup, Denmark), and biotinylated antibodies were from Vector Laboratories (CA, USA).

Anti-Human CD47 Antibody Preparation

Anti-human CD47 (B6H12.2) hybridoma was obtained from ATCC (MD, USA). Hybridoma cells were cultured, and the antibody was purified by protein G following the standard protocol [7].

Flow Cytometry

The protein expressions on cell surface were verified by flow cytometry (LSR II flow cytometer, BD Biosciences, CA, USA). Data were analyzed by FlowJo software (Tree Star, OR, USA).

Preparation of Human Macrophages

Primary human monocyte-derived macrophages (MDMs) were prepared as previously described [25]. Informed consent was obtained from healthy volunteers before drawing blood. The study protocol was reviewed and approved by the Kumamoto University Medical Ethical Committee (Rinri No. 420). Macrophages were induced by either 10 ng/ml GM-CSF or 100 ng/ml M-CSF in 10% FBS-RPMI1640.

For macrophage differentiation, MDMs were stimulated as described in [26]: 1) M1, by 100 ng/ml LPS and 20 ng/ml IFN-γ; 2) M2, by 20 ng/ml IL-4; or 3) tumor-associated macrophage (TAM)–like MDM, by M-CSF and KKU-213–conditioned media (CM).

In Vitro Phagocytosis Assay

The macrophage phagocytic activity was accessed as in [7]. Briefly, MDMs were plated into a glass-bottom dish (Greiner Bio-One, Frickenhausen, Germany). The indicated antibodies (10 μg/ml) were added concomitantly with CFSE-labeled CCA cells (E:T ratio = 1:4). Before analysis, nuclei of the adherent cells were stained by Hoechst 33342. The images were taken by the BZ-8100 Biozero fluorescent microscope and were quantified by BZ-II Analyzer (Keyence, Osaka, Japan). Data are presented as the phagocytic index calculated as the number of phagocytosed $CSFE^+$/Hoechst 33342 stained cells per 100 MDM.

Transplenic Intrahepatic Metastasis Mouse Model and Anti-CD47 Treatment In Vivo

mCherry-expressing KKU-213 (5×10^5 cells) [27] were intrasplenically injected into 8- to 10-week-old NOD Rag-2/Jak3 double-deficient mice (NRJ mice) (n = 8/group) [28] as described in [29] with minor modification. For this study, spleen was kept intact and served as a primary site, whereas the liver was a metastatic site. Anti-CD47 treatment was administered intravenously at 200 μg/mouse on day 3

and was on every third day thereafter. Mice weights were monitored to evaluated the animals' health. On day 27, livers and spleens were removed and weighed. Fluorescent signals were analyzed by the Maestro *in vivo* fluorescent imaging system using Maestro 2.10.0 software (CRi, MA, USA). The anterior and posterior right liver lobes were used for immunohistochemistry.

Mice were housed and monitored in the animal research facility according to institutional guidelines. All protocols were approved by the Institutional Animal Care and Use Committee, Kumamoto University, Japan.

Immunohistochemistry

The CD47 expression in cancer tissues was detected by immunohistochemical staining with the standard protocol. Signals were enhanced using EnVision-system-HRP (Dako). The expressions of CD47 were evaluated using the H-score according to the standard procedure [30] by two independent evaluators.

For mouse tissue evaluation, F4/80 (representing infiltrating macrophage) and CK19 (representing CCA cells) expressions were determined in consecutive tumor sections from liver and spleen. Signals were amplified by Vectastain Elite ABC standard kit (Vector Laboratories). The F4/80-positive and CK19-positive areas were quantified by Image J as described previously [31]. Percentage of macrophage per cancer area was calculated as follows: %macrophage/cancer area = (F4/80-positive area)/(CK-19–positive area)*100.

Measurement of Cytokine Secretion by Antibody Array

Cytokines from resting and TAM-like macrophages were analyzed by Human Cytokine Array C3 (Ray Biotech, GA, USA). Signals were measured using an ImageQuant LAS 4000 system and ImageQuant TL software (GE Healthcare, Uppsala, Sweden). The signal from an individual spot on a membrane exposed to TAM-like-CM was normalized by positive controls prior to normalization with corresponding spots on resting macrophage membrane.

IL-6 and IL-10 ELISA

IL-6 and IL-10 levels in CMs of resting and TAM-like macrophages were measured by ELISA kits for IL-6 (eBioscience) and IL-10 (Biolegend). Absorbance at 450 nm was determined using an iMark microplate reader (Bio-Rad, Hercules, CA, USA). KKU-213-CM was used as reference.

Statistical Analysis

Data was expressed as mean ± SD, unless otherwise indicated. Significant differences between experimental groups were determined by the Mann-Whitney test using GraphPad Prism version 6.07 (CA, USA). $P < 0.05$ was considered significant.

Results

CD47 Expressions in CCA and HCC

CD47 expressions were determined in two liver cancers; CCA and HCC, in both tissues and cell lines. CD47 were detected in 54 CCAs and 22 HCCs, and their expressions were recorded as H-scores. CCAs expressed higher CD47 compared to HCCs (Figure 1*A*). Only 2 HCC tissues (9.1%) expressed detectable CD47, while CD47 was not detected in 4 CCAs (7.4%). The cell line results were similar; 3 CCAs (KKU-055, KKU-213, and HuCCT1) highly expressed CD47, and only KKU-100 CCA and 2 HCCs (HepG2 and Huh7) expressed lower CD47 (Figure 1*B*). Thus, CCAs universally expressed high CD47.

CD47 Protected CCA from Macrophage Phagocytosis, and These Effects Were Interrupted by Disrupting CD47-SIRPα Interaction

High CD47 in CCA prompted us to examine its effects on CCA phagocytosis. The effects of CD47 against macrophage-mediated phagocytosis were determined in KKU-100 (low CD47) and KKU-213 (high CD47). The results showed higher phagocytic activity against KKU-100. Anti-CD47 antibody could not promote the macrophage-mediated phagocytosis of KKU-100 but did so for KKU-213 (Supplement Figure 1*A*). Similar results were obtained when the phagocytic activities were determined in anti-CD47 treated KKU-055 and HuCCT1 (Supplement Figure 1*B*). These results imply that high CD47-expressed CCA cells are promising targets for anti-CD47 treatment. KKU-213 was selected as a representative CCA cell line.

We next tested whether the effects observed in anti-CD47 were specific. Two clones of anti-CD47 antibodies were selected: B6H12.2 (CD47 blocking antibody) and 2D3 (CD47 nonblocking antibody) [7]. Treatment with B6H12.2 enhanced the macrophage-mediated phagocytosis of KKU-213 when compared to 2D3 or control IgG. The results were consistent when MDMs from three volunteers were used (Figure 1*C*).

We further tested the effects of SIRPα blockage on macrophage-mediated CCA phagocytosis. Anti-SIRPα SE5A5 potentiated macrophage phagocytosis against KKU-213 at a level comparable with anti-CD47 B6H12.2 (Figure 1*D*). These results indicated that disrupting CD47-SIRPα interaction enhanced the macrophage-mediated phagocytosis of CCA.

Anti-CD47 Treatment Reduced CCA Colonization in Both Primary and Metastatic Sites

To validate the effects of CD47 targeting in CCA, NRJ mice were intrasplenically injected with mCherry-expressing KKU-213. Anti-CD47 (B6H12.2) was given through tail vein for eight doses. The weights of spleens and livers from the anti-CD47 group were significantly lower than those of controls (n = 8/group) (Figure 2, *A* and *B*). Consistently, fluorescent signals in the spleens and livers were significantly reduced in the anti-CD47 group (Figure 2, *C* and *D*). No serious adverse effects were observed (Supplement Figure 2).

The effects of anti-CD47 treatment were further assessed by immunohistochemistry (Figure 2, *E* and *F*). The results showed that CCA colonization was less of a burden in both organs of the anti-CD47 group, while F4/80-positive cell infiltration seemed to be higher. The percentage of macrophage per cancer area was semiquantitatively determined (n = 4/group). The results showed that the % macrophage/cancer area seemed to be higher in both liver and spleen; however, only those observed in liver reached statistical significance. To emphasize the cancer-diminishing effect of anti-CD47, the % CK19-positive area per liver lobes per mouse was measured in the anterior and posterior right liver lobes (n = 4/group). The results showed a significant reduction of cancer colonization in anti-CD47 group (Figure 2*I*).

Anti-CD47 Antibody Potentiated Resting, M1, M2, and TAM-Like Phagocytosis

The effects of anti-CD47 B6H12.2 on M1 and M2 are recognized [7,32]. However, increased TAM infiltration is expected in the cancer microenvironment [13]. We identified the effects of anti-CD47–

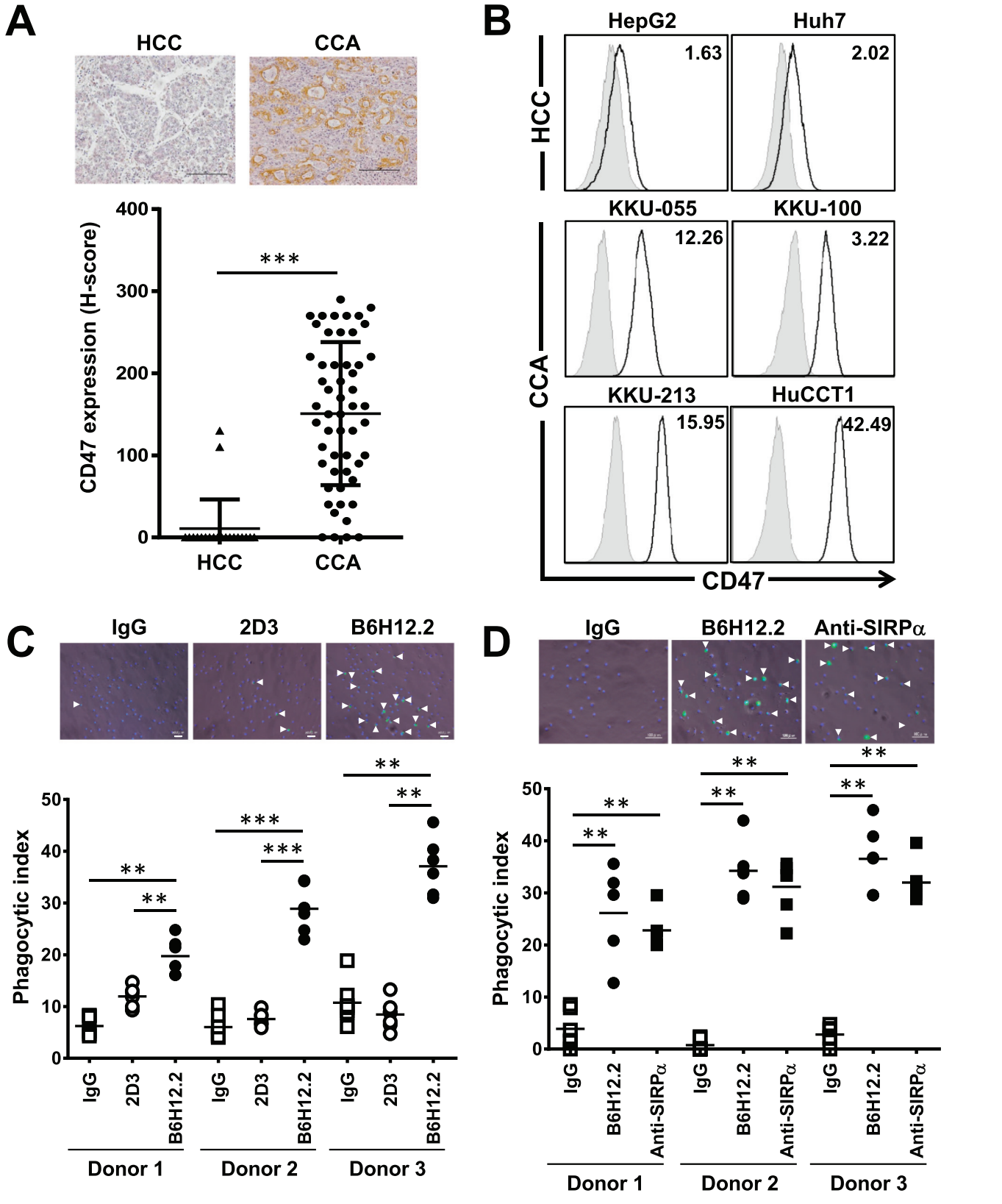

Figure 1. High CD47 expressions protected CCA from macrophage phagocytosis, and these effects were abolished by disrupting CD47-SIRPα interaction. (A) Expressions of CD47 in HCC (▲) and CCA (●) tissues were expressed by H-score. Each spot represents an individual sample. Representative pictures of HCC and CCA are shown. Bar = 100 μm. (B) CD47 expressions in HCC (HepG2 and Huh7) and CCA (KKU-055, KKU-100, KKU-213, and HuCCT1) cell lines were determined by flow cytometry. White histogram represents anti-CD47–stained cells, while gray histogram represents isotype control staining. Numbers on upper-right corners are the mean fluorescent intensities (MFI) of anti-CD47–stained cells normalized by those of isotype control. (C) Phagocytic indices of anti-CD47 blocking antibody (B6H12.2) treatment compared to nonblocking antibody (2D3). (D) Comparison of anti-CD47 (B6H12.2) and anti-SIRPα (SE5A5) treatments. Representative pictures of phagocytic cells are presented with phagocytosed cells indicated by the arrow heads. IgG was isotype control IgG. $^{**}P < .01$, $^{***}P < .001$.

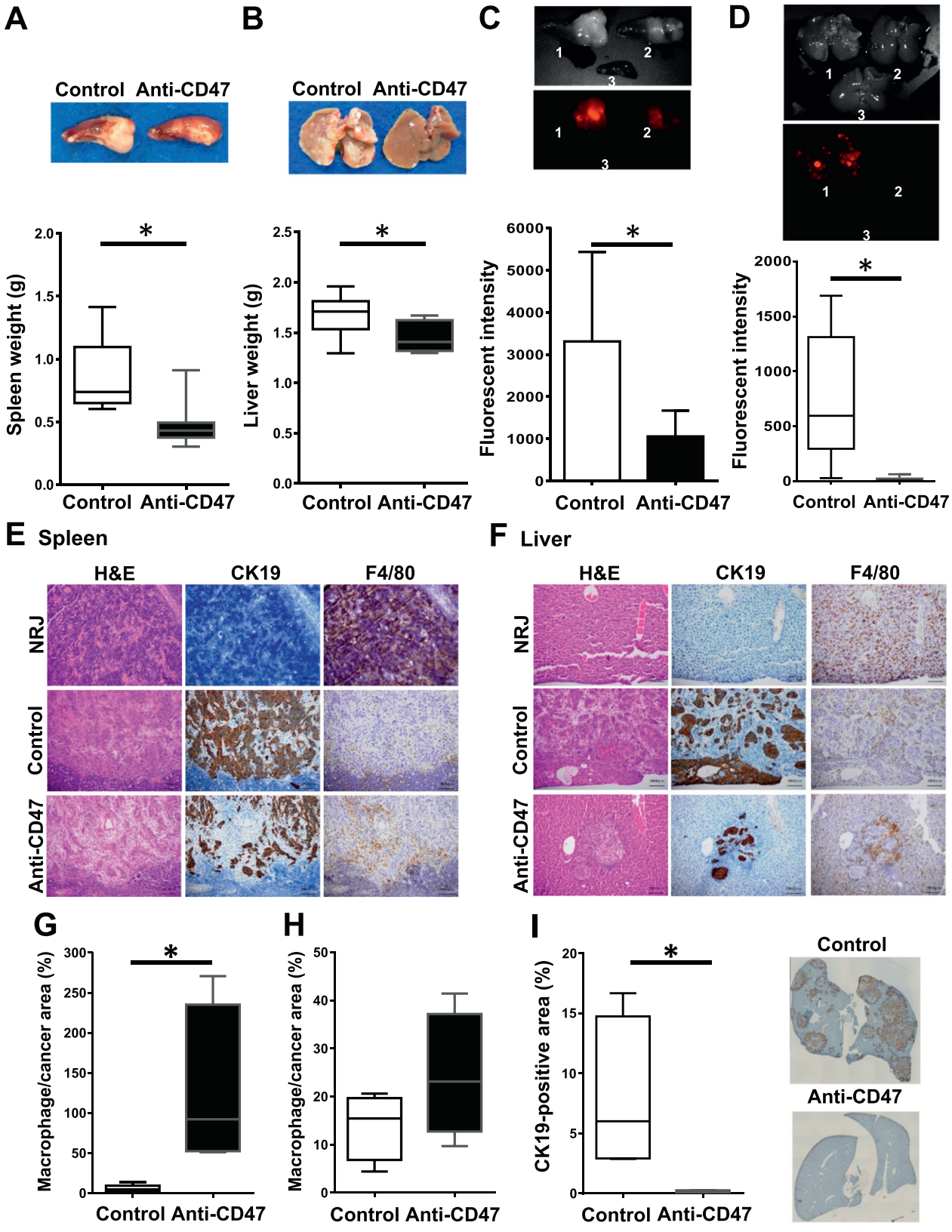

Figure 2. Anti-CD47 treatment reduced cancer colonization in spleen and liver but increased macrophage infiltration. Splenic (A) and liver (B) weights of mice in control (white box) and anti-CD47–treated group (black box) are presented. Red fluorescent intensities per time (total counts/second) detected from spleens (C) and livers (D) are shown. Representative images are presented in small insets. 1 = control, 2 = anti-CD47 treated, 3 = non–cancer-injected (NRJ) organ. Hematoxylin and eosin and immunohistochemistry staining of CK19 (bile duct marker) and F4/80 (mouse macrophage marker) is demonstrated in spleen (E) and liver (F). NRJ = corresponding area of spleen and liver from NRJ mouse not injected with CCA cells. Bar = 100 μm. Percentages of macrophage per cancer area in spleens (G) and livers (H) of control and anti-CD47–treated group are presented (n = 4/group). (I) % CK19-positive area in anterior and posterior right lobes of livers from both groups (n = 4/group). Small insets show representative images of livers. Bars show minimum to maximum numbers. *P < .05.

mediated TAM phagocytosis. MDMs were differentiated into M1, M2, and TAM-like subtypes. Comparing to GM-CSF–induced macrophages, M-CSF–induced MDMs (resting) were more spindle-like shaped, and TAM-like MDMs acquired a similar shape to resting and M2 macrophages (Supplement Figure 3*A*). The surface markers of macrophage subpopulations were validated (n = 5 donors/group). As shown in Supplement Figure 3*B*, TAM-like MDMs expressed higher CD14, CD163, and CD206 but lower CD86. Expressions of SIRPα were low in all M-CSF–induced macrophages when compared to GM-CSF–induced ones. No significant differences in HLA-DR were observed in the current study.

To elucidate roles of anti-CD47 B6H12.2 on macrophage subpopulation phagocytosis, anti-CD47 was applied together with CSFE-labeled KKU-213. Anti-CD47 stimulated all macrophage subpopulation-mediated CCA phagocytosis (Figure 3, *A* and *B*, n = 4 volunteers). The phagocytic index of control IgG-treated TAM-like MDM seemed to be lower than in other groups, but this did not reach statistical significance. Interestingly, anti-CD47 increased the phagocytic indices of resting, M1, M2, and TAM-like MDMs 10.2-, 3.6-, 4.0-, and 17.0-fold when normalized to those of control IgG.

CCA-CM altered macrophage cytokine productions

Phenotypic alterations and decreased phagocytic activities in TAM-like MDM (Supplement Figure 3*B* and Figure 3*B*) led us to speculate the CCA-modulated surrounding macrophage functions. Forty-two cytokines were checked in CM from TAM-like and resting macrophages (Figure 4*A*). Nine cytokines including IL-6, MCP-2, MCP-3, CXCL-5, GROα, angiogenin (ANG), GRO a/b/g, IL-8, and IL-10 were increased in TAM-like-CM (Figure 4*B*).

To verify the cytokine alterations, IL-6 and IL-10 were determined by ELISA using macrophage-CM from two donors. IL-6 was not detected in resting macrophages but was 76.5 ± 2.0 and 535.8 ± 8.8 ng/ml in TAM-like MDMs and 31.6 ± 1.6 ng/ml in KKU-213-CM (Figure 4*C*). IL-10 was not detectable in KKU-213-CM but was 8.7 ± 0.04 and 11.9 ± 0.18 ng/ml in resting and 28.0 ± 0.4 and 38.1 ± 0.20 ng/ml in TAM-like-CM (data were expressed as

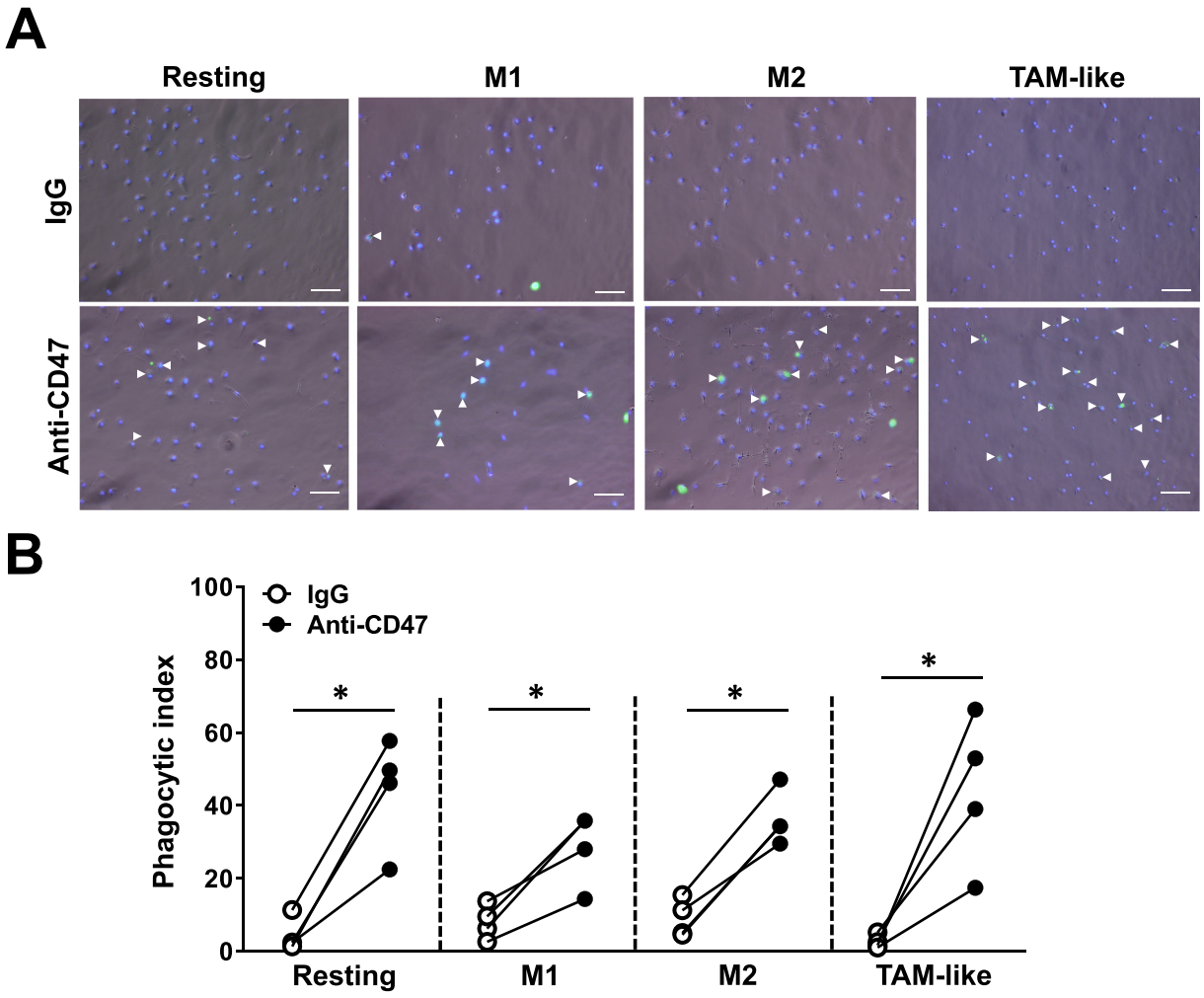

Figure 3. Treatment with anti-CD47 antibody potentiated the phagocytic activities of all macrophage subgroups. (A) Representative images of CCA-phagocytosed resting, M1, M2, and TAM-like subgroups. Arrowheads indicated phagocytosed cells in isotype control IgG- and anti-CD47–treated groups. Bar = 100 μm. (B) Phagocytic indices of IgG- (○) and anti-CD47–treated (●) resting, M1, M2, and TAM-like MDMs. Individual spots each represent the mean phagocytic index from an individual donor. Line compared the phagocytic indices from the same donor. *P < .05.

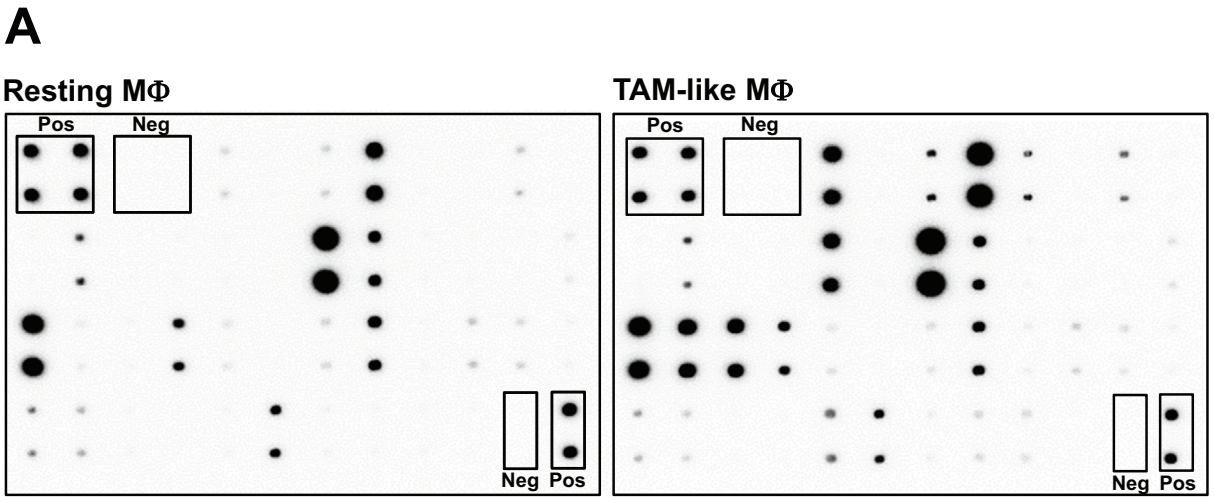

	A	B	C	D	E	F	G	H	I	J	K	L
1	Pos	Pos	Neg	Neg	CXCL5	G-CSF	GM-CSF	GRO a/b/g	GRPα (CXCL1)	CCL1	IL-1α	IL-1β
2												
3	IL-2	IL-3	IL-4	IL-5	IL-6	IL-7	IL-8	IL-10	IL-12	IL-13	IL-15	IFN-γ
4												
5	MCP-1 (CCL2)	MCP-2 (CCL8)	MCP-3 (CCL7)	M-CSF	MDC (CCL22)	MIG (CXCL9)	MIP-1δ	RANTES (CCL5)	SCF	SDF-1	TARC (CCL17)	TGFβ1
6												
7	TNFα	TNFβ	EGF	IGF-1	Angiogenin	OSM	TPO	VEGF-A	PDGF-BB	Leptin	Neg	Pos
8												

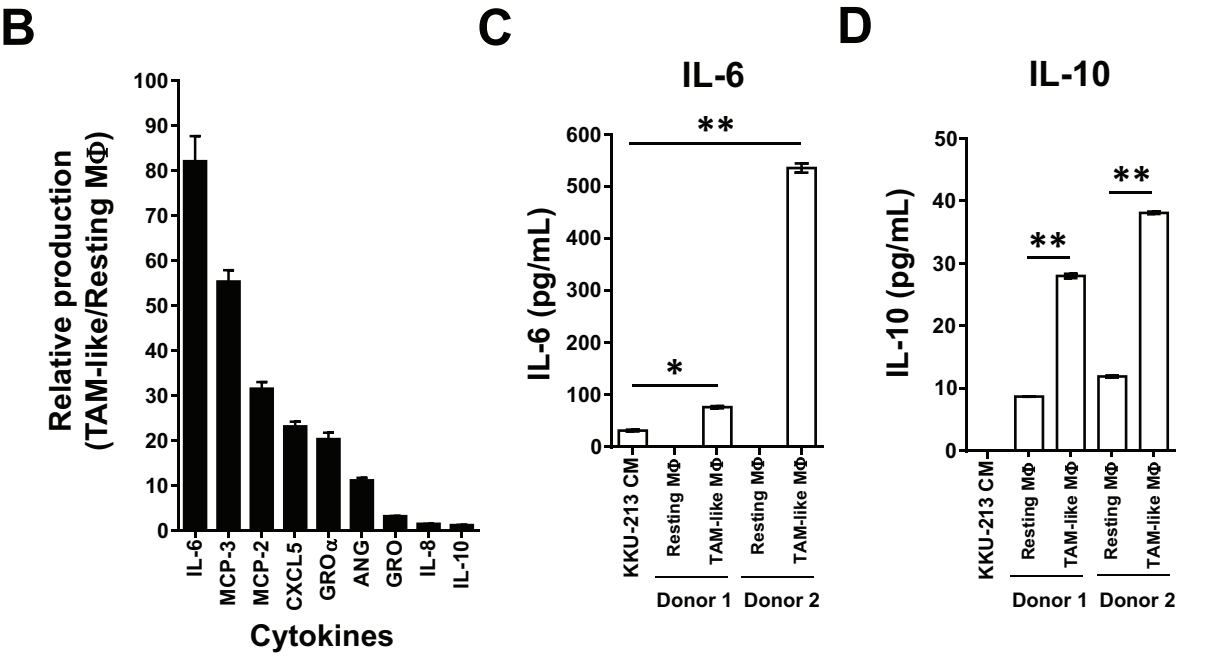

Figure 4. Treatment with KKU-213-CM promoted macrophage-produced cancer-promoting cytokines. (A) Cytokines released in resting macrophage-CM (resting MΦ) and TAM-like-CM (TAM-like MΦ) detected by cytokine arrays. Pos = positive control spots, Neg = negative control spots. (B) Increased cytokines in TAM-like MDM are demonstrated by relative production (normalized intensities in TAM-like/resting MΦ). IL-6 (C) and IL-10 (D) were validated in macrophage subgroups from two donors. KKU-213-CM was used as reference. $^{**}P < .01$.

mean ± SEM, Figure 4*D*). These results confirmed that IL-6 and IL-10 were upregulated in TAM-like MDM.

Discussion

Promising results of immune checkpoint therapy have enlightened multiple devastated cancer outcomes. The therapeutic potential of CD47 signal in cancers has been demonstrated [7,26,32]. Blockage of CD47-SIRPα binding-enhanced phagocytosis might be appropriate for chronic inflammation-related and TAM-associated CCA [13,20,33]. We demonstrated that CD47 was highly expressed in CCA compared to HCC. Disruption of CD47-SIRPα interaction by blocking antibodies promoted macrophage-mediated phagocytosis.

The benefit of anti-CD47 was highlighted in a liver metastatic model. Promotion of macrophage infiltration was suggested as a mechanism of anti-CD47–mediated cancer eradication. It was suggested for the first time in this study that products secreted in CCA modulated macrophages toward M2-like cancer-promoting properties and anti-CD47 could abolish these properties and promote TAM-like MDM phagocytosis. Therefore, the high CD47 in CCA provides an opportunity for targeting treatment. CD47 blockage will challenge macrophage, including TAM, leading to modulation and promotion of CCA elimination.

We demonstrated high expressions of CD47 in CCA but not HCC. These results were consistent with the previous report demonstrating marginal CD47 expressions in HCC [34]. CD47 was generally high in most CCAs, suggesting a significant role. Thus, the importance of CD47 in CCA was determined, and the results suggested that CD47 corresponds inversely to macrophage phagocytic activity. The relationship between CD47 level and its immune protective role was previously demonstrated [35]. We demonstrated that anti-CD47 antibody could promote phagocytosis of CCA with high CD47 expression but not in a borderline-expressing one (KKU-100). This was consistent with a report on primary effusion lymphoma [35] but differed from reports on HCC [34,36] that showed anti-CD47 potentiated phagocytosis of HCC with marginal CD47 expression. These discriminate results might be due to low SIRPα expression in our MDM or variations in macrophage activities from different sources. The factors that influence macrophage phagocytic activities are beyond the scope of the present study.

The potential use of CD47 as a target for treatment was demonstrated. Treatment with anti-CD47 B6H12.2 specifically increased macrophage phagocytic activities. The comparable effects of CD47 and SIRPα blockage suggested the possible utility of anti-CD47 and the newly developed SIRPα blockers [37]. The advantage of anti-CD47 was emphasized *in vivo*, with multiple liver colonies of cancer mimicking CCA in the commonly diagnosed advanced stage [21,38]. NRJ lacks mature B, T, and NK as well as complement proteins [28]. *Sirpa* polymorphism in NOD-related mouse promotes human CD47 binding and prevents phagocytosis of CD47-expressed human cancer cells [39,40]. Thus, this mouse is suitable for demonstrating anti-CD47–mediated macrophage phagocytosis. The results showed dramatic differences in cancer colonization, demonstrated by reductions in organ weights, fluorescent signals, and % CK19-positive areas. Increased infiltrations of mouse macrophages were also observed. This was in agreement with a report on the effect of CD47 blockage on macrophage recruitment promotion [26,32,34].

The mechanism by which anti-CD47 suppressed CCA growth and metastasis in our model is proposed to be mainly through the induction of macrophage phagocytosis. However, multiple macrophage subpopulations have been demonstrated [41]. Therefore, the effects of anti-CD47 on macrophage subgroups were determined. Macrophage subpopulations were generated [26], and phenotypic alterations were checked. TAM-like MDM showed high CD14, CD163, and CD206 but low SIRPα and CD86. High CD163 and CD206 were similar to the M2c subpopulation [42,43]. Moreover, our results demonstrated for the first time that anti-CD47 potentiated the phagocytic activities of all macrophage subpopulations. Anti-CD47 effects on resting, M1, and M2 were reported [7,26,32,36], and the effect of anti-CD47 on TAM was proposed [7]. TAM is presumably a major population in cancer, and hence, the effects would be through TAM modulation. Our result suggested that anti-CD47 promotes all macrophage subgroup-mediated cancer phagocytosis.

As we observed altered phenotypes and phagocytic activities in TAM-like MDM, we hypothesized that CCA alters macrophage to be cancer promoting. We showed that cytokine production including IL-6, MCP-2, MCP-3, CXCL-5, GROα, ANG, GRO a/b/g, IL-8, and IL-10 was increased in TAM-like MDM. Elevations of CXCL5, IL-6, and IL-8 and their contributions to dismal prognosis of CCA were reported [15,17,44]. IL-6 and GROα from CCA-stimulated mesenchymal cells promoted CCA growth [45], and IL-10 from CCA promoting CCA progression were shown [46]. The induction of MCP-2 in M-CSF–induced MDM has been reported [47], and we showed higher MCP-2 in TAM-like MDM. ANG promoted prostate cancer growth, and angiogenesis was noted [48]. Taken together, our results suggested that macrophage exposed to CCA-CM or TAM-like MDM might be an alternative source of cytokines that could promote CCA. The effects of MCP-2, MCP-3, and ANG have never been clarified in CCA and require attention.

High expression of CD47 in CCA was demonstrated in this study. The effectiveness of CD47-SIRPα blockage for macrophage-mediated CCA removal was proven *in vitro* and *in vivo*. Anti-CD47–promoted phagocytosis was independent of the macrophage subtypes and could overcome TAM-promoting cancer effects. Altogether, these that suggested CD47-SIRPα interaction might be a novel promising target for precision treatment of CCA.

Acknowledgements

We thank Ms. Y. Kanagawa for her secretarial work.

Appendix A. Supplementary Data

Supplementary data to this article can be found online at https://doi.org/10.1016/j.tranon.2018.10.007.

References

[1] Brown EJ and Frazier WA (2001). Integrin-associated protein (CD47) and its ligands. *Trends Cell Biol* **11**(3), 130–135.

[2] Matozaki T, Murata Y, Okazawa H, and Ohnishi H (2009). Functions and molecular mechanisms of the CD47-SIRPalpha signalling pathway. *Trends Cell Biol* **19**(2), 72–80.

[3] Sick E, Jeanne A, Schneider C, Dedieu S, Takeda K, and Martiny L (2012). CD47 update: a multifaceted actor in the tumour microenvironment of potential therapeutic interest. *Br J Pharmacol* **167**(7), 1415–1430.

[4] Oldenborg PA, Zheleznyak A, Fang YF, Lagenaur CF, Gresham HD, and Lindberg FP (2000). Role of CD47 as a marker of self on red blood cells. *Science* **288**(5473), 2051–2054.

[5] Jaiswal S, Jamieson CH, Pang WW, Park CY, Chao MP, Majeti R, Traver D, van Rooijen N, and Weissman IL (2009). CD47 is upregulated on circulating hematopoietic stem cells and leukemia cells to avoid phagocytosis. *Cell* **138**(2), 271–285.

[6] Majeti R, Chao MP, Alizadeh AA, Pang WW, Jaiswal S, Gibbs Jr KD, van Rooijen N, and Weissman IL (2009). CD47 is an adverse prognostic factor and therapeutic antibody target on human acute myeloid leukemia stem cells. *Cell* **138**(2), 286–299.

[7] Willingham SB, Volkmer JP, Gentles AJ, Sahoo D, Dalerba P, Mitra SS, Wang J, Contreras-Trujillo H, Martin R, and Cohen JD, et al (2012). The CD47-signal regulatory protein alpha (SIRPa) interaction is a therapeutic target for human solid tumors. *Proc Natl Acad Sci U S A* **109**(17), 6662–6667.

[8] Ring NG, Herndler-Brandstetter D, Weiskopf K, Shan L, Volkmer JP, George BM, Lietzenmayer M, McKenna KM, Naik TJ, and McCarty A, et al (2017). Anti-SIRPalpha antibody immunotherapy enhances neutrophil and macrophage antitumor activity. *Proc Natl Acad Sci U S A* **114**(49), E10578-10585.

[9] Mukkamalla SKR, Naseri HM, Kim BM, Katz SC, and Armenio VA (2018). Trends in incidence and factors affecting survival of patients with cholangiocarcinoma in the United States. *J Natl Compr Cancer Netw* **16**(4), 370–376.

[10] Witjes CD, Karim-Kos HE, Visser O, de Vries E, JN IJ, de Man RA, Coebergh JW, and Verhoef C (2012). Intrahepatic cholangiocarcinoma in a low endemic area: rising incidence and improved survival. *HPB (Oxford)* **14**(11), 777–781.

[11] Khuntikeo N, Titapun A, Loilome W, Yongvanit P, Thinkhamrop B, Chamadol N, Boonmars T, Nethanomsak T, Andrews RH, and Petney TN, et al (2018). Current perspectives on opisthorchiasis control and cholangiocarcinoma detection in Southeast Asia. *Front Med (Lausanne)* **5**, 117.

[12] Patel T (2014). New insights into the molecular pathogenesis of intrahepatic cholangiocarcinoma. *J Gastroenterol* **49**(2), 165–172.

[13] Subimerb C, Pinlaor S, Khuntikeo N, Leelayuwat C, Morris A, McGrath MS, and Wongkham S (2010). Tissue invasive macrophage density is correlated with prognosis in cholangiocarcinoma. *Mol Med Rep* **3**(4), 597–605.

[14] Subimerb C, Pinlaor S, Lulitanond V, Khuntikeo N, Okada S, McGrath MS, and Wongkham S (2010). Circulating CD14(+) CD16(+) monocyte levels predict tissue invasive character of cholangiocarcinoma. *Clin Exp Immunol* **161**(3), 471–479.

[15] Sun Q, Li F, Sun F, and Niu J (2015). Interleukin-8 is a prognostic indicator in human hilar cholangiocarcinoma. *Int J Clin Exp Pathol* **8**(7), 8376–8384.

[16] Asukai K, Kawamoto K, Eguchi H, Konno M, Nishida N, Koseki J, Noguchi K, Hasegawa S, Ogawa H, and Yamada D, et al (2015). Prognostic impact of peritumoral IL-17-positive cells and IL-17 axis in patients with intrahepatic cholangiocarcinoma. *Ann Surg Oncol* **22**(Suppl. 3), S1524–S1531.

[17] Sripa B, Thinkhamrop B, Mairiang E, Laha T, Kaewkes S, Sithithaworn P, Periago MV, Bhudhisawasdi V, Yonglitthipagon P, and Mulvenna J, et al (2012). Elevated plasma IL-6 associates with increased risk of advanced fibrosis and cholangiocarcinoma in individuals infected by Opisthorchis viverrini. *PLoS Negl Trop Dis* **6**(5)e1654.

[18] Sawada R, Ku Y, Akita M, Otani K, Fujikura K, Itoh T, Ajiki T, Fukumoto T, Kakeji Y, and Zen Y (2018). Interleukin-33 overexpression reflects less aggressive tumour features in large-duct type cholangiocarcinomas. *Histopathology* **73**(2), 259–272.

[19] Bridgewater J, Galle PR, Khan SA, Llovet JM, Park JW, Patel T, Pawlik TM, and Gores GJ (2014). Guidelines for the diagnosis and management of intrahepatic cholangiocarcinoma. *J Hepatol* **60**(6), 1268–1289.

[20] Banales JM, Cardinale V, Carpino G, Marzioni M, Andersen JB, Invernizzi P, Lind GE, Folseraas T, Forbes SJ, and Fouassier L, et al (2016). Expert consensus document: cholangiocarcinoma: current knowledge and future perspectives consensus statement from the European Network for the Study of Cholangiocarcinoma (ENS-CCA). *Nat Rev Gastroenterol Hepatol* **13**(5), 261–280.

[21] Tan JC, Coburn NG, Baxter NN, Kiss A, and Law CH (2008). Surgical management of intrahepatic cholangiocarcinoma—a population-based study. *Ann Surg Oncol* **15**(2), 600–608.

[22] Sangkhamanon S, Jongpairat P, Sookprasert A, Wirasorn K, Titapun A, Pugkhem A, Ungareevittaya P, and Chindaprasirt J (2017). Programmed death-ligand 1 (PD-L1) expression associated with a high neutrophil/lymphocyte ratio in cholangiocarcinoma. *Asian Pac J Cancer Prev* **18**(6), 1671–1674.

[23] Fontugne J, Augustin J, Pujals A, Compagnon P, Rousseau B, Luciani A, Tournigand C, Cherqui D, Azoulay D, and Pawlotsky JM, et al (2017). PD-L1 expression in perihilar and intrahepatic cholangiocarcinoma. *Oncotarget* **8**(15), 24644–24651.

[24] Ma YH, Dou WT, Pan YF, Dong LW, Tan YX, He XP, Tian H, and Wang HY (2017). Fluorogenic 2D peptidosheet unravels CD47 as a potential biomarker for profiling hepatocellular carcinoma and cholangiocarcinoma tissues. *Adv Mater* **29**(5).

[25] Chihara T, Suzu S, Hassan R, Chutiwitoonchai N, Hiyoshi M, Motoyoshi K, Kimura F, and Okada S (2010). IL-34 and M-CSF share the receptor Fms but are not identical in biological activity and signal activation. *Cell Death Differ* **17**(12), 1917–1927.

[26] Zhang Y, Sime W, Juhas M, and Sjolander A (2013). Crosstalk between colon cancer cells and macrophages via inflammatory mediators and CD47 promotes tumour cell migration. *Eur J Cancer* **49**(15), 3320–3334.

[27] Vaeteewoottacharn K, Kariya R, Dana P, Fujikawa S, Matsuda K, Ohkuma K, Kudo E, Kraiklang R, Wongkham C, and Wongkham S, et al (2016). Inhibition of carbonic anhydrase potentiates bevacizumab treatment in cholangiocarcinoma. *Tumour Biol* **37**(7), 9023–9035.

[28] Goto H, Kariya R, Shimamoto M, Kudo E, Taura M, Katano H, and Okada S (2012). Antitumor effect of berberine against primary effusion lymphoma via inhibition of NF-kappaB pathway. *Cancer Sci* **103**(4), 775–781.

[29] Zender L, Spector MS, Xue W, Flemming P, Cordon-Cardo C, Silke J, Fan ST, Luk JM, Wigler M, and Hannon GJ, et al (2006). Identification and validation of oncogenes in liver cancer using an integrative oncogenomic approach. *Cell* **125**(7), 1253–1267.

[30] Fitzgibbons PL, Bradley LA, Fatheree LA, Alsabeh R, Fulton RS, Goldsmith JD, Haas TS, Karabakhtsian RG, Loykasek PA, and Marolt MJ, et al (2014). Principles of analytic validation of immunohistochemical assays: Guideline from the College of American Pathologists Pathology and Laboratory Quality Center. *Arch Pathol Lab Med* **138**(11), 1432–1443.

[31] Jung KY, Cho SW, Kim YA, Kim D, Oh BC, Park DJ, and Park YJ (2015). Cancers with higher density of tumor-associated macrophages were associated with poor survival rates. *J Pathol Transl Med* **49**(4), 318–324.

[32] Zhang M, Hutter G, Kahn SA, Azad TD, Gholamin S, Xu CY, Liu J, Achrol AS, Richard C, and Sommerkamp P, et al (2016). Anti-CD47 treatment stimulates phagocytosis of glioblastoma by M1 and M2 polarized macrophages and promotes M1 polarized macrophages in vivo. *PLoS One* **11**(4)e0153550.

[33] Hasita H, Komohara Y, Okabe H, Masuda T, Ohnishi K, Lei XF, Beppu T, Baba H, and Takeya M (2010). Significance of alternatively activated macrophages in patients with intrahepatic cholangiocarcinoma. *Cancer Sci* **101**(8), 1913–1919.

[34] Xiao Z, Chung H, Banan B, Manning PT, Ott KC, Lin S, Capoccia BJ, Subramanian V, Hiebsch RR, and Upadhya GA, et al (2015). Antibody mediated therapy targeting CD47 inhibits tumor progression of hepatocellular carcinoma. *Cancer Lett* **360**(2), 302–309.

[35] Goto H, Kojima Y, Matsuda K, Kariya R, Taura M, Kuwahara K, Nagai H, Katano H, and Okada S (2014). Efficacy of anti-CD47 antibody-mediated phagocytosis with macrophages against primary effusion lymphoma. *Eur J Cancer* **50**(10), 1836–1846.

[36] Lo J, Lau EY, So FT, Lu P, Chan VS, Cheung VC, Ching RH, Cheng BY, Ma MK, and Ng IO, et al (2016). Anti-CD47 antibody suppresses tumour growth and augments the effect of chemotherapy treatment in hepatocellular carcinoma. *Liver Int* **36**(5), 737–745.

[37] Yanagita T, Murata Y, Tanaka D, Motegi SI, Arai E, Daniwijaya EW, Hazama D, Washio K, Saito Y, and Kotani T, et al (2017). Anti-SIRPalpha antibodies as a potential new tool for cancer immunotherapy. *JCI Insight* **2**(1)e89140.

[38] Luvira V, Nilprapha K, Bhudhisawasdi V, Pugkhem A, Chamadol N, and Kamsa-ard S (2016). Cholangiocarcinoma patient outcome in Northeastern Thailand: single-center prospective study. *Asian Pac J Cancer Prev* **17**(1), 401–406.

[39] Takenaka K, Prasolava TK, Wang JC, Mortin-Toth SM, Khalouei S, Gan OI, Dick JE, and Danska JS (2007). Polymorphism in Sirpa modulates engraftment of human hematopoietic stem cells. *Nat Immunol* **8**(12), 1313–1323.

[40] Yamauchi T, Takenaka K, Urata S, Shima T, Kikushige Y, Tokuyama T, Iwamoto C, Nishihara M, Iwasaki H, and Miyamoto T, et al (2013). Polymorphic Sirpa is the genetic determinant for NOD-based mouse lines to achieve efficient human cell engraftment. *Blood* **121**(8), 1316–1325.

[41] Mantovani A, Sozzani S, Locati M, Allavena P, and Sica A (2002). Macrophage polarization: tumor-associated macrophages as a paradigm for polarized M2 mononuclear phagocytes. *Trends Immunol* **23**(11), 549–555.

[42] Yuan A, Hsiao YJ, Chen HY, Chen HW, Ho CC, Chen YY, Liu YC, Hong TH, Yu SL, and Chen JJ, et al (2015). Opposite effects of M1 and M2 macrophage subtypes on lung cancer progression. *Sci Rep* **5**14273.

[43] Murdoch C, Muthana M, Coffelt SB, and Lewis CE (2008). The role of myeloid cells in the promotion of tumour angiogenesis. *Nat Rev Cancer* **8**(8), 618–631.

[44] Okabe H, Beppu T, Ueda M, Hayashi H, Ishiko T, Masuda T, Otao R, Horlad H, Mima K, and Miyake K, et al (2012). Identification of CXCL5/ENA-78 as a factor involved in the interaction between cholangiocarcinoma cells and cancer-associated fibroblasts. *Int J Cancer* **131**(10), 2234–2241.

[45] Haga H, Yan IK, Takahashi K, Wood J, Zubair A, and Patel T (2015). Tumour cell-derived extracellular vesicles interact with mesenchymal stem cells to modulate the microenvironment and enhance cholangiocarcinoma growth. *J Extracell Vesicles* **4**24900.

[46] Thepmalee C, Panya A, Junking M, and Chieochansin T (2018). PT Yenchitsomanus, Inhibition of IL-10 and TGF-beta receptors on dendritic cells enhances activation of effector T-cells to kill cholangiocarcinoma cells. *Hum Vaccin Immunother* , 1–9.

[47] Sierra-Filardi E, Nieto C, Dominguez-Soto A, Barroso R, Sanchez-Mateos P, Puig-Kroger A, Lopez-Bravo M, Joven J, Ardavin C, and Rodriguez-Fernandez JL, et al (2014). CCL2 shapes macrophage polarization by GM-CSF and M-CSF: identification of CCL2/CCR2-dependent gene expression profile. *J Immunol* **192**(8), 3858–3867.

[48] Yoshioka N, Wang L, Kishimoto K, Tsuji T, and Hu GF (2006). A therapeutic target for prostate cancer based on angiogenin-stimulated angiogenesis and cancer cell proliferation. *Proc Natl Acad Sci U S A* **103**(39), 14519–14524.